

# Implicit Likelihood Inference of the Neutrino Mass Hierarchy from Cosmological Data

Ke Wang<sup>1\*</sup>

<sup>1</sup>*Department of Physics, Liaoning Normal University, Dalian 116029, China*

(Dated: December 22, 2025)

In this paper, we turn to the Learning the Universe Implicit Likelihood Inference (LtU-ILI) pipeline to perform a multi-round ILI of the neutrino mass hierarchy from cosmological data, including  $TT$ ,  $TE$ ,  $EE$  power spectra of Planck 2018 and distance ratios of DESI DR2. More precisely, we first embed the CMB power spectra simulator **CLASS** into the LtU-ILI pipeline. And then, opting for Sequential Neural Likelihood Estimation (SNLE), we sequentially train neural networks using 2 rounds of 5000 simulations to target a “black box” likelihood of our forward model with one additional neutrino mass hierarchy parameter  $\hat{\Delta}$  and six base cosmological parameters. We find that  $\hat{\Delta} = 0.12216^{+0.26193}_{-0.29243}$  (68%CL) which slightly prefers  $\hat{\Delta} > 0$ , hence the normal hierarchy.

## I. INTRODUCTION

Neutrino oscillation experiments require that there are three distinct mass eigenstates with the differences of squared neutrino masses as [1]

$$\Delta m_{21}^2 = m_2^2 - m_1^2 = 7.5 \times 10^{-5} \text{eV}^2, \quad (1)$$

$$|\Delta m_{31}^2| = |m_3^2 - m_1^2| = 2.45 \times 10^{-3} \text{eV}^2. \quad (2)$$

Since all neutrino mass eigenstates are supposed to be sufficiently light  $< 1\text{eV}$ , these massive cosmic neutrinos would be relativistic and behave as the radiation in the early universe, while they would change to be non-relativistic and contribute to the matter budget in the late universe. This transition would leave footprints in the cosmological expansion history [2]. Furthermore, also in the late universe, the large thermal velocities of non-relativistic neutrinos would suppress the growth of structure below the neutrino free-streaming scale [2]. Therefore, the combination of the cosmic microwave background (CMB, Planck 2018 [3]), the baryon acoustic oscillation (BAO, DESI DR2 [4]) and the matter power spectrum [5] can impose a tight constraint on the neutrino masses, hence the neutrino mass hierarchy. For example, the combination of Planck, ACT [6] and DESI DR2 provides a strong constraint,  $\sum m_\nu < 0.077\text{eV}$  (95%CL) [7]. This constraint becomes excessively tighter by including recent SPT-3G data [8],  $\sum m_\nu < 0.048\text{eV}$  (95%CL). Such strong bounds are consistent with the preference for the normal hierarchy  $m_1 < m_3$  from [9].

To implement the inference of the neutrino masses and other cosmological parameters from observations by the traditional explicit likelihood inference, even for CMB data from Planck 2018 [3] only, one should turn to the low- $\ell$  temperature-only **Commander** likelihood to deal with the temperature power spectrum in the multipole range  $2 \leq \ell \leq 29$ , the low- $\ell$  EE likelihood from **SimAll** to deal with  $EE$ -polarization power spectrum in the multipole range  $2 \leq \ell \leq 29$ , the **Plik** high-multipole likelihood

to deal with  $TT$ ,  $TE$  and  $EE$  angular power spectra at multipoles  $\ell \geq 30$  and the CMB lensing likelihood to deal with the CMB lensing-potential power spectrum, respectively. However, the above 4 likelihood patches only represent the summary statistics of CMB anisotropies map. If any extension to the base- $\Lambda$ CDM model or any update of the data combination occurs, the likelihoods should be modified more or less accordingly. Especially for extensions with a lot of parameters or data requiring large numbers of nuisance parameters, the traditional explicit likelihood inference performs poorly.

Implicit Likelihood Inference (ILI) [10], also known as simulation-based inference (SBI) and likelihood-free inference (LFI), is a novel alternative that can learn the statistical relationship between parameters and data by machine learning (ML). Due to the prohibitive computational cost of  $N$ -body simulation [11–13], the training data in question are usually obtained before ILI and compressed to summary statistics, such as power spectrum [14], bispectrum [15], marked power spectrum [16], skew spectrum [17], wavelet statistics [18] and field-level statistics [19]. However, **CLASS** [20] and **CAMB** [21] as CMB simulators are efficient. Therefore, given an initial wider cosmological parameter priors, these CMB simulators can forward-simulate sets of parameter values to the training data of  $TT$ ,  $TE$ ,  $EE$  and CMB lensing-potential power spectra. After the first round of training, the obtained posteriors serve as the new priors for the second round of training, and so on. This sequential learning has been applied to ILI of the cosmological parameters from CMB [22].

ILI of neutrino masses from BOSS voids obtains a modest constraint on  $\sum m_\nu$  [23]. In this paper, we also do not expect a strong limit on  $\sum m_\nu$  from the combination of DESI DR2 [4] and Planck 2018 [3] excluding the CMB lensing-potential power spectrum, and we only perform ILI of the neutrino mass hierarchy by sequential learning. To study the preference for what neutrino mass hierarchy directly, we extend the base- $\Lambda$ CDM model with the neutrino mass hierarchy parameter [24, 25]

$$\Delta = \frac{m_3 - m_1}{m_1 + m_3}, \quad (3)$$

where  $\Delta > 0$  for the normal hierarchy and  $\Delta < 0$  for the

\*wangke@lnnu.edu.cn

inverted hierarchy respectively.

This paper is organized as follows. In Section II, we introduce the CMB power spectra simulator including the neutrino mass hierarchy parameter. In Section III, we perform a multi-round ILI of the neutrino mass hierarchy. Finally, a brief summary and discussion are provided in Section IV.

## II. CMB POWER SPECTRA SIMULATOR

The neutrino mass hierarchy parameter  $\Delta$  is related to the total neutrino mass as [24, 25]

$$\sum m_\nu = \sqrt{\frac{|\Delta m_{31}^2|}{|\Delta|}} + \sqrt{\frac{(1-\Delta)^2}{4|\Delta|} |\Delta m_{31}^2| + \Delta m_{21}^2}. \quad (4)$$

Therefore, the usual upper limits on  $\sum m_\nu$  mean that  $\Delta$  should have a U-shaped distribution, as hinted at by the left subplot of Fig. 1. This total non-Gaussian U-shaped posterior maybe can not be estimated from the data correctly. Here, we introduce a new parameter  $\tilde{\Delta} = -\text{sign}(\Delta) \times \lg(|\Delta|)$  which is related to  $\sum m_\nu$  as the right subplot of Fig. 1. Consequently, an upper limit on  $\sum m_\nu$  would be equivalent to a  $\lceil$ -shaped posterior of  $\tilde{\Delta}$ . Taking  $\tilde{\Delta}$  into account, our cosmological model has 7 free parameters. Since we will turn to the sequential learning, their initial uniform priors can be wider

$$\boldsymbol{\theta} = \begin{Bmatrix} \omega_b \\ \omega_c \\ 100\theta_s \\ \ln(10^{10} A_s) \\ n_s \\ \tau \\ \tilde{\Delta} \end{Bmatrix} = \begin{Bmatrix} \mathcal{U}(0.020, 0.024) \\ \mathcal{U}(0.11, 0.13) \\ \mathcal{U}(1.036, 1.044) \\ \mathcal{U}(2.98, 3.10) \\ \mathcal{U}(0.94, 1.02) \\ \mathcal{U}(0.04, 0.08) \\ \mathcal{U}(-3, 3) \end{Bmatrix}. \quad (5)$$

As the procedure of [22], the CMB simulator is constructed by three steps. 1) Given the prior  $\mathcal{P}(\boldsymbol{\theta})$ , we can draw sets of candidate parameter values from it and forward-simulate these values to the corresponding CMB power spectra  $C_\ell^{XX'}(\boldsymbol{\theta})$  ( $X = T, E$ ) by the Einstein-Boltzmann solver CLASS [20]. 2) For the Planck experiment, its noise spectrum can be mimicked by the contributions of a Gaussian white noise and a Gaussian beam [26]

$$N_\ell^{XX'} = \delta_{XX'} \theta_{\text{FWHM}}^2 \sigma_X^2 \exp\left(\ell(\ell+1) + \frac{\theta_{\text{FWHM}}^2}{8 \ln 2}\right), \quad (6)$$

where  $\theta_{\text{FWHM}}$  is the full width at half maximum of a Gaussian beam and  $\sigma_X$  is the detector sensitivity. Thanks to `fake_planck_realistic` within `MontePython` [27], a ready-made  $N_\ell^{XX'}$  for Planck's temperature and polarization measurements, we have

$\bar{C}_\ell^{XX'}(\boldsymbol{\theta}) = C_\ell^{XX'}(\boldsymbol{\theta}) + N_\ell^{XX'}$ . 3) Given the covariance matrix

$$\begin{pmatrix} \bar{C}_\ell^{TT}(\boldsymbol{\theta}) & \bar{C}_\ell^{TE}(\boldsymbol{\theta}) \\ \bar{C}_\ell^{TE}(\boldsymbol{\theta}) & \bar{C}_\ell^{EE}(\boldsymbol{\theta}) \end{pmatrix}, \quad (7)$$

the Gaussian distributions of the multipole coefficients  $a_{\ell m}^X$  of CMB maps can be sampled accordingly. For a specific couple of  $\ell'$  and  $m'$ , if the corresponding covariance matrix block is decomposed into the product of a lower triangular matrix  $L$  and its conjugate transpose  $L^T$  using the Cholesky decomposition,  $a_{\ell' m'}^X$  can be sampled as

$$\begin{pmatrix} a_{\ell' m'}^T \\ a_{\ell' m'}^E \end{pmatrix} = L(\boldsymbol{\theta}) \begin{pmatrix} \mathcal{N}(0, 1) \\ \mathcal{N}(0, 1) \end{pmatrix}. \quad (8)$$

According to the estimator of power spectra

$$\hat{C}_\ell^{XX'}(\boldsymbol{\theta}) = \frac{1}{2\ell+1} \sum_{m=-\ell}^{\ell} a_{\ell m}^{X*} a_{\ell m}^{X'}, \quad (9)$$

there obviously is a fundamental uncertainty (due to cosmic variance) in the knowledge about the power spectra. More precisely,  $\hat{C}_\ell^{XX'}(\boldsymbol{\theta})$  has a Wishart distribution at low  $\ell$  and tends towards a multivariate Gaussian distribution at large  $\ell$  [28]. For simplicity, at  $\ell > 52$ , we set  $\hat{C}_\ell^{XX'}(\boldsymbol{\theta}) = \bar{C}_\ell^{XX'}(\boldsymbol{\theta}) + n_\ell^{XX'}(\boldsymbol{\theta}^0)$ , where  $n_\ell^{XX'}(\boldsymbol{\theta}^0)$  depends on a fiducial cosmology<sup>1</sup> and can be simply sampled from the corresponding multivariate normal distribution with the covariance matrix

$$\frac{2}{2\ell+1} \times \begin{pmatrix} (\bar{C}_\ell^{TT}(\boldsymbol{\theta}^0))^2 & \bar{C}_\ell^{TT}(\boldsymbol{\theta}^0) \bar{C}_\ell^{TE}(\boldsymbol{\theta}^0) & (\bar{C}_\ell^{TE}(\boldsymbol{\theta}^0))^2 \\ & \frac{1}{2} \left( \bar{C}_\ell^{TT}(\boldsymbol{\theta}^0) \bar{C}_\ell^{TE}(\boldsymbol{\theta}^0) + (\bar{C}_\ell^{TE}(\boldsymbol{\theta}^0))^2 \right) & \\ \bar{C}_\ell^{TE}(\boldsymbol{\theta}^0) \bar{C}_\ell^{TE}(\boldsymbol{\theta}^0) & \bar{C}_\ell^{TT}(\boldsymbol{\theta}^0) \bar{C}_\ell^{EE}(\boldsymbol{\theta}^0) & \bar{C}_\ell^{TE}(\boldsymbol{\theta}^0) \bar{C}_\ell^{EE}(\boldsymbol{\theta}^0) \\ & & + (\bar{C}_\ell^{EE}(\boldsymbol{\theta}^0))^2 \\ (\bar{C}_\ell^{TE}(\boldsymbol{\theta}^0))^2 & \bar{C}_\ell^{TE}(\boldsymbol{\theta}^0) \bar{C}_\ell^{EE}(\boldsymbol{\theta}^0) & (\bar{C}_\ell^{EE}(\boldsymbol{\theta}^0))^2 \end{pmatrix}. \quad (10)$$

In Fig. 2, we compare  $C_\ell^{XX'}(\boldsymbol{\theta}^0)$ ,  $\bar{C}_\ell^{XX'}(\boldsymbol{\theta}^0)$  and  $\hat{C}_\ell^{XX'}(\boldsymbol{\theta}^0)$  respectively.

As for the BAO simulator, given the covariance matrix of distance ratios of DESI DR2 [4], the noise realizations are sampled from the corresponding multivariate normal distribution.

<sup>1</sup> Here we directly download the theoretical power spectra of the best-fit model  $C_\ell^{XX'}$  from Planck 2018 [29], which can also be reproduced by a specific set of parameters  $\boldsymbol{\theta}^0 = \{\omega_b, \omega_c, 100\theta_s, \ln(10^{10} A_s), n_s, \tau\} = \{0.02237, 0.1200, 1.04092, 3.044, 0.9649, 0.0544\}$ .

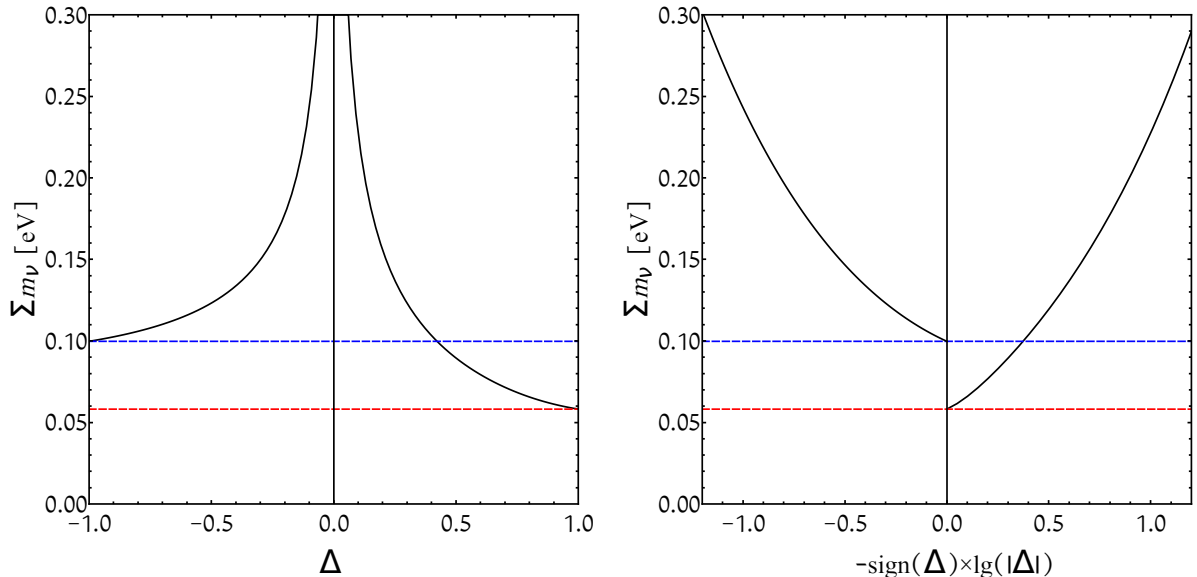


FIG. 1: The total neutrino mass  $\sum m_\nu$  as a function of  $\Delta$  (left) or  $\tilde{\Delta} = -\text{sign}(\Delta) \times \lg(|\Delta|)$  (right), according to which an upper limit on  $\sum m_\nu$  can be derived from a U-shaped posterior of  $\Delta$  or a  $\cap$ -shaped posterior of  $\tilde{\Delta}$ .

### III. MULTI-ROUND ILI OF THE NEUTRINO MASS HIERARCHY

In this paper, we turn to the Learning the Universe Implicit Likelihood Inference (LtU-ILI) pipeline [30], where the computational backend is set as `sbi` [31], a PyTorch [32] package, and the sequential analog of Neural Likelihood Estimation (SNLE) [33, 34] is chosen as the inference engine. The loss function for NLE is

$$\mathcal{L} = -\mathbb{E}_{\mathcal{D}_{\text{train}}}[\ln q_{\mathbf{w}}(\mathbf{x}|\boldsymbol{\theta})], \quad (11)$$

where  $\mathbf{w}$  is the network weights, the expectation  $\mathbb{E}_{\mathcal{D}_{\text{train}}}$  is taken over all data-parameter pairs  $\{(\mathbf{x}_i, \boldsymbol{\theta}_i)\}$  in the training data set  $\mathcal{D}_{\text{train}}$  and  $q_{\mathbf{w}}(\mathbf{x}|\boldsymbol{\theta})$  is converging to the likelihood through the minimization of  $\mathcal{L}$  over  $\mathbf{w}$ . Then, we sequentially perform 2 rounds of training. In each round, we train an NLE model with 5000 simulated data-parameter pairs  $\{(\mathbf{x}_i, \boldsymbol{\theta}_i)\}$  by an ensemble of 4 Neural Density Estimations [34] (NDEs), each using a Masked Autoregressive Flow [35] (MAF) architecture with 50 hidden features and 5 transformations.

After the last round of training, the learned likelihood is related to an amortized posterior as  $\mathcal{P}(\boldsymbol{\theta}|\mathbf{x}) \propto q_{\mathbf{w}}(\mathbf{x}|\boldsymbol{\theta})\mathcal{P}(\boldsymbol{\theta})$ . Due to the local amortization of  $\mathcal{P}(\boldsymbol{\theta}|\mathbf{x})$ , the marginal posterior of  $\boldsymbol{\theta}$  can be sampled from  $\mathcal{P}(\boldsymbol{\theta}|\mathbf{x})$  without retraining, for any  $\mathbf{x}$  drawn from the initial prior. Moreover, local amortization allows for special validation tests that are not accessible to traditional explicit likelihood inference, such as the rank statistics, the marginal percentile coverage test and the direct comparison between true and predicted parameter values. Similarly to the training data set  $\mathcal{D}_{\text{train}}$ , we prepare 500 data-parameter pairs  $\{(\mathbf{x}_i, \boldsymbol{\theta}_i)\}$  as the testing data set

$\mathcal{D}_{\text{test}}$ .  $\mathcal{D}_{\text{test}}$  was not used in the SNLE training, but their marginal posteriors are sampled according to the local amortization of  $\mathcal{P}(\boldsymbol{\theta}|\mathbf{x})$  for the following validation.

Given a data-parameter pair  $\{(\mathbf{x}_i, \boldsymbol{\theta}_i)\}$  from  $\mathcal{D}_{\text{test}}$ , we can count the rank of each given parameter  $\theta_i$  in its  $N$  posterior samples

$$\{\theta'_1, \theta'_2, \dots, \theta'_{N=400}\} \sim \mathcal{P}(\boldsymbol{\theta}|\mathbf{x}_i), \quad \forall (\mathbf{x}_i, \boldsymbol{\theta}_i) \in \mathcal{D}_{\text{test}}. \quad (12)$$

If the true posterior is estimated exactly, the rank statistic of  $\theta_i$  in  $\mathcal{D}_{\text{test}}$  should be distributed uniformly. This is almost the case for our cosmological parameters, as shown in Fig. 3. Replacing the rank with the cumulative density function (CDF) value, the distribution of the latter one would also be uniformly distributed

$$\int_{-\infty}^{\theta_i} d\theta \mathcal{P}(\boldsymbol{\theta}|\mathbf{x}_i) \sim \mathcal{U}(0, 1), \quad \forall (\mathbf{x}_i, \boldsymbol{\theta}_i) \in \mathcal{D}_{\text{test}}. \quad (13)$$

In the percentile-percentile (P-P) plot, Fig. 4, we compare the CDF of the distribution of all CDF values calculated at  $(\mathbf{x}_i, \boldsymbol{\theta}_i) \in \mathcal{D}_{\text{test}}$  with the CDF of  $\mathcal{U}(0, 1)$ . The good agreement between each couple of distributions means that our learned posteriors are almost globally consistent with the truth. Finally, in Fig. 5, we directly compare the true value of  $\theta_i$  in  $\mathcal{D}_{\text{test}}$  and the corresponding predicted values sampled from  $\mathcal{P}(\boldsymbol{\theta}|\mathbf{x}_i)$ . For a large  $|\tilde{\Delta}|$ , or a large  $\sum m_\nu$  according to Fig. 1, cosmological data can not distinguish the normal hierarchy and the inverted hierarchy. So given a large true  $|\tilde{\Delta}|$ , its predicted one can be either  $> 0$  or  $< 0$ , as shown in the last subplot in Fig. 5. As  $|\tilde{\Delta}|$  is decreasing, the hierarchy preference occurs.

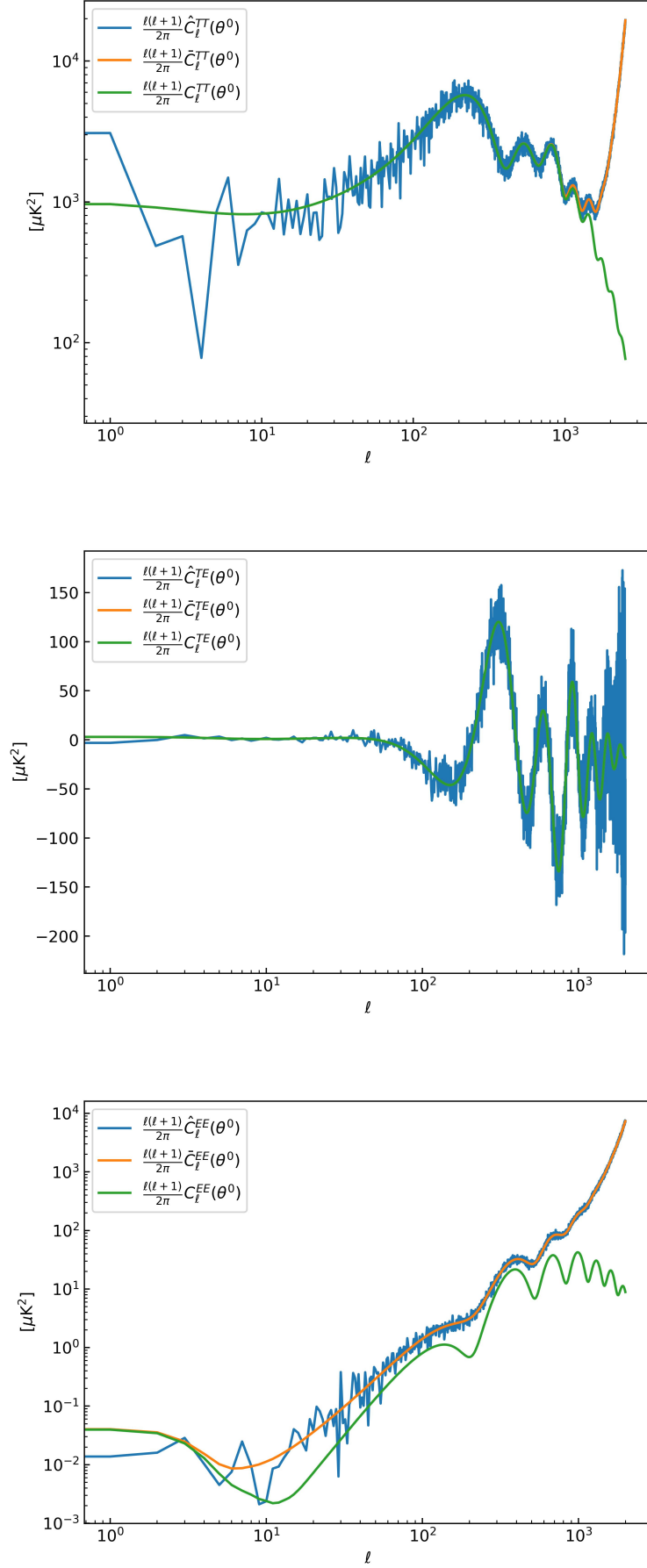


FIG. 2: Comparison among  $C_\ell^{XX'}(\theta^0)$ ,  $\bar{C}_\ell^{XX'}(\theta^0)$  and  $\hat{C}_\ell^{XX'}(\theta^0)$  respectively, where  $\theta^0$  does not include the neutrino mass hierarchy parameter  $\tilde{\Delta}$ .

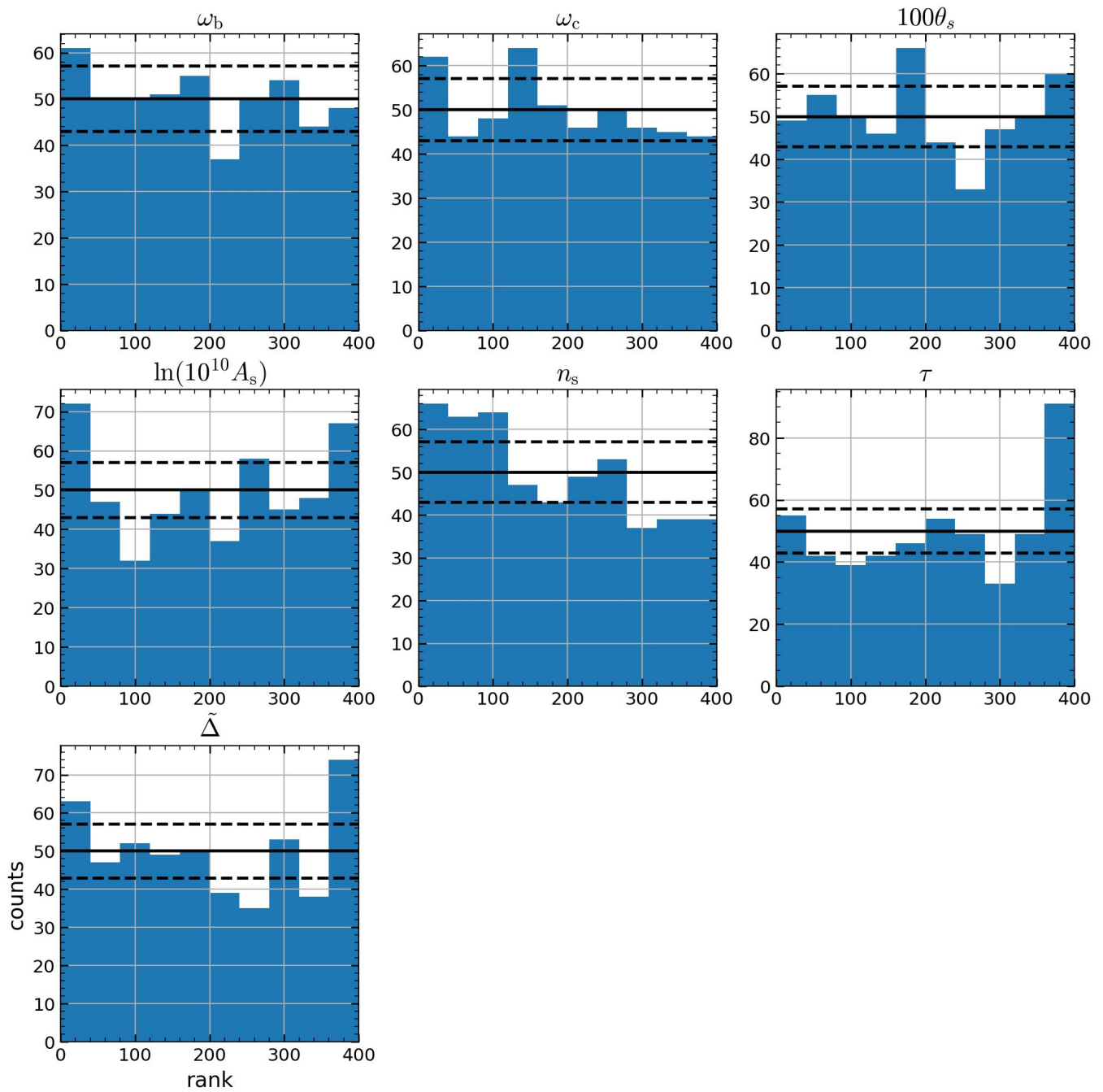


FIG. 3: Rank statistic of each parameter, where the number of samples is  $N = 400$  and the testing data set  $\mathcal{D}_{\text{test}}$  includes 500 data-parameter pairs.

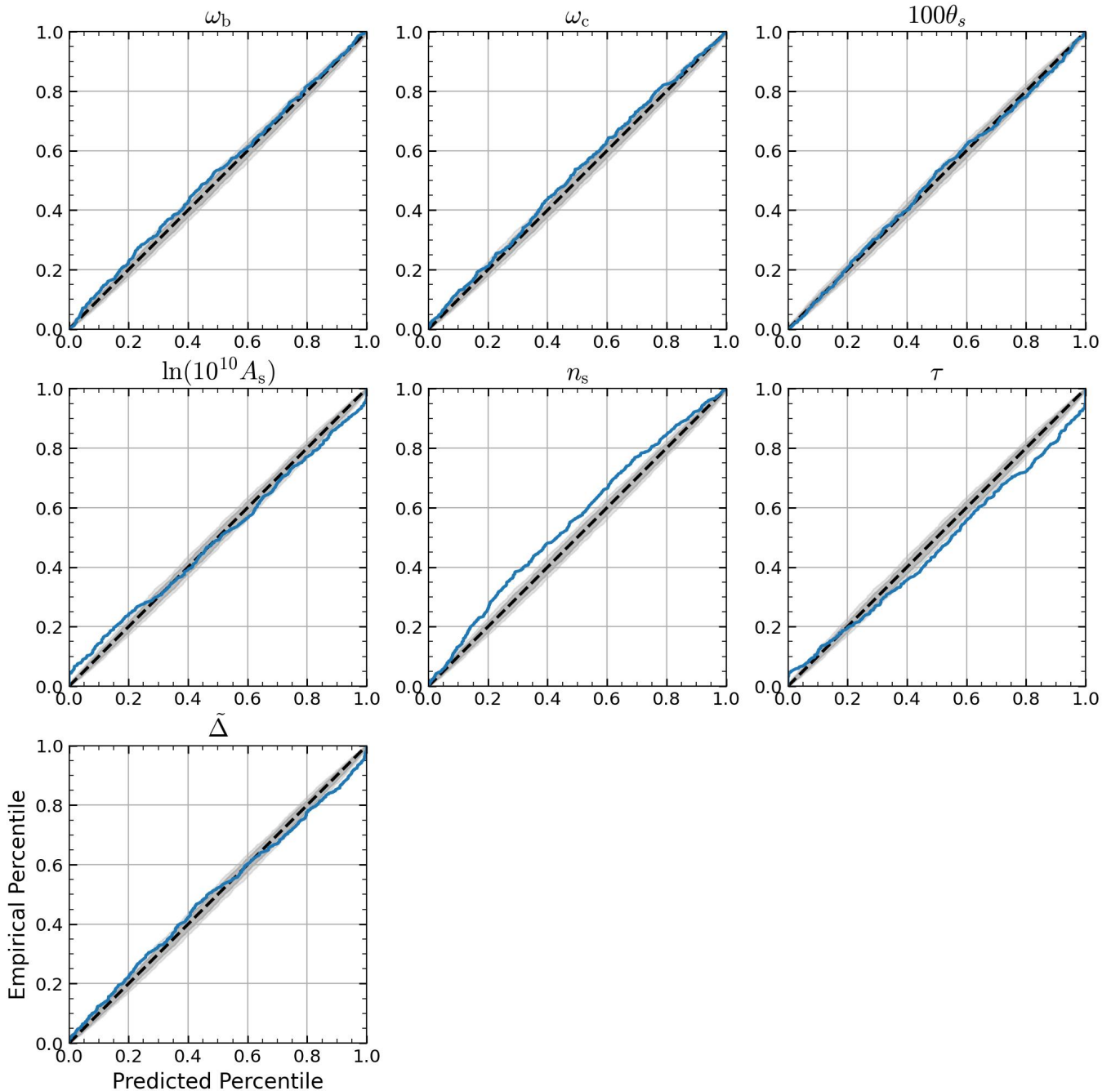


FIG. 4: Marginal percentile coverage test for cosmological parameters, where the empirical percentile from uniform distribution  $\mathcal{U}(0, 1)$  and the predicted percentile from the distribution of all CDF values calculated at  $(\mathbf{x}_i, \theta_i) \in \mathcal{D}_{\text{test}}$  as Eq. (13).

After validation by  $\mathcal{D}_{\text{test}}$ , we now consider the observed cosmological data  $\mathbf{x}_o$ , including the observed CMB spectra and their uncertainties `COM_PowerSpect_CMB_XX'` from Planck 2018 [29] and the distance ratios and their covariance matrix of DESI DR2 [4]. Given the amortized posterior  $\mathcal{P}(\boldsymbol{\theta}|\mathbf{x})$ , the posterior for  $\mathbf{x}_o$  can then be obtained through the usual Monte Carlo Markov Chain sampling which we perform with `emcee` [36], as shown

in Fig. 6. Constraints on the base cosmological parameters are consistent with Planck 2018 [3], except a little larger  $\ln(10^{10}A_s)$  and  $\tau$ . That is to say, for these two parameters, our ILI does not behave as well as the Planck low- $\ell$  EE likelihood `SimAll` on large scales. If the CMB lensing-potential power spectrum is considered, the performance of ILI should be improved. The constraint on the neutrino mass hierarchy parameter is

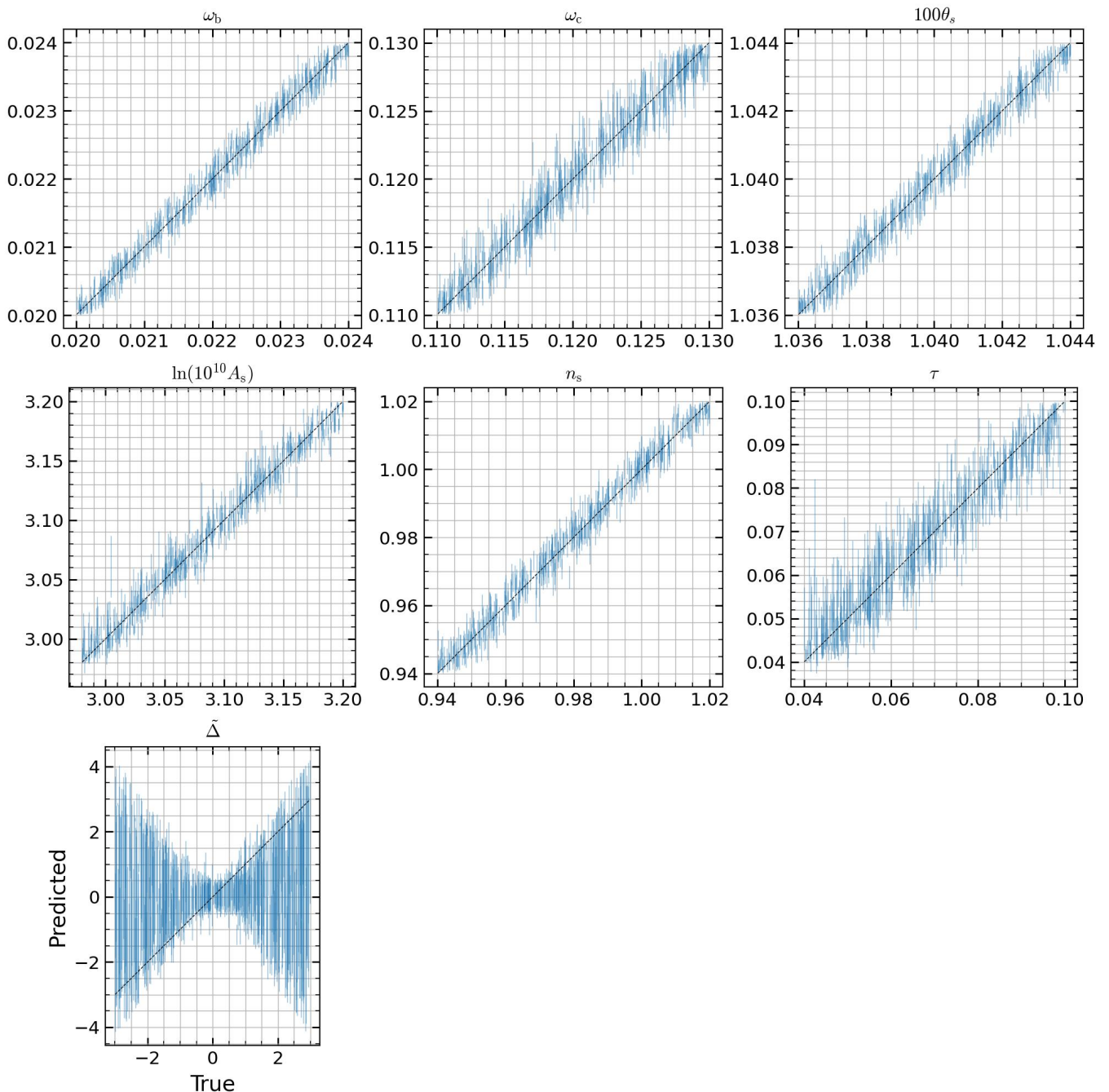


FIG. 5: Comparison between true and predicted value of cosmological parameters.

$\tilde{\Delta} = 0.12216^{+0.26193}_{-0.29243}$  (68%CL). According to its definition, the preference for  $\tilde{\Delta} > 0$  means that the normal hierarchy is favored.

#### IV. SUMMARY AND DISCUSSION

In this paper, we first construct the CMB power spectra simulator  $\hat{C}_\ell^{XX'}(\boldsymbol{\theta})$  by decorating the CLASS outputs  $C_\ell^{XX'}(\boldsymbol{\theta})$  with the noise realizations of Planck experiment and the fundamental uncertainties due to cosmic variance. Then, SNLE is chosen as the inference engine to target an amortized posterior  $\mathcal{P}(\boldsymbol{\theta}|\mathbf{x})$  indirectly. Af-

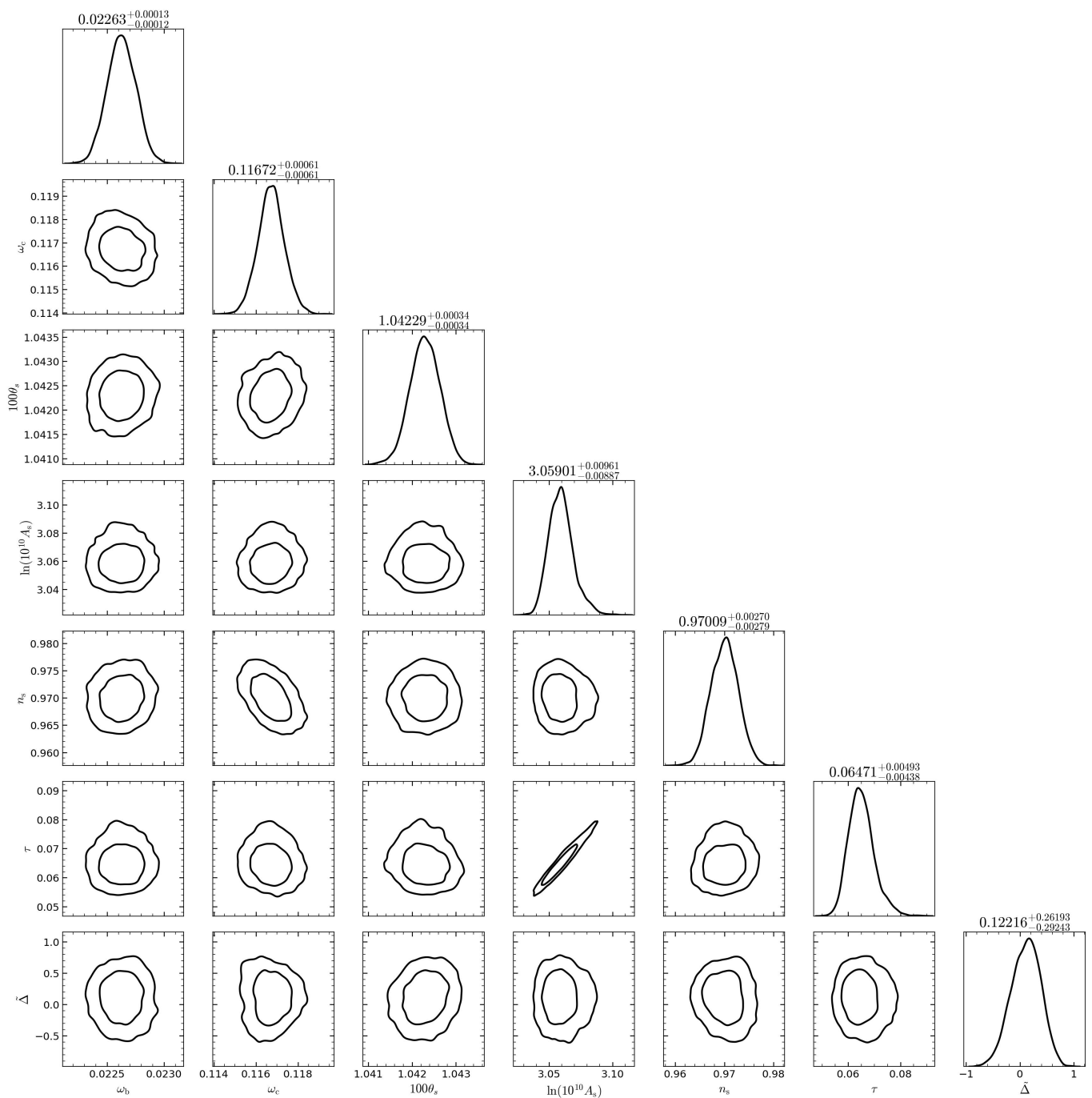


FIG. 6: Posterior distribution of  $\theta$  inferred from the combination of DESI DR2 [4] and Planck 2018 [3] excluding the CMB lensing-potential power spectrum, where 68% interval of each parameter is displayed as the titles of diagonal subplots and contours contain 68% and 95% of the probability.

ter training neural networks with  $\mathcal{D}_{\text{train}}$ , we perform the validation test with the rank statistics, the P-P plot and the percentile coverage plot of  $\mathcal{D}_{\text{test}}$ . Given the credible learned  $\mathcal{P}(\theta|\mathbf{x})$ ,  $\mathcal{P}(\theta|\mathbf{x}_0)$  is sampled with `emcee` [36], where  $\mathbf{x}_0$  stands for the the observed cosmological data including Planck 2018 [29] and DESI DR2 [4]. Finally, we

find that  $\tilde{\Delta} = 0.12216^{+0.26193}_{-0.29243}$  (68%CL), which slightly prefers  $\tilde{\Delta} > 0$ , hence the normal hierarchy.

As we know,  $TT$ ,  $EE$  and  $TE$  angular power spectra are just three summary statistics of CMB anisotropies map. In fact, there exist other CMB summary statistics, such as the lensing-potential power spectrum [37],

temperature and polarization angular bispectra and even the next higher-order non-Gaussianity (NG) correlation function, i.e., the CMB angular trispectra [38]. In particular, embedding the simulators of the lensing-potential power spectrum or the cross-correlations between CMB lensing and other large-scale structure observations [39, 40] into ILI should impose stronger constraints on the neutrino masses and their hierarchy. We will do this in future work. For some summary statistics, their explicit likelihoods are ready-made or the construc-

tion of their simulators is difficult than the built of their explicit likelihoods. In these cases, the explicit likelihoods can be embedded into ILI through their effective simulators [41].

**Acknowledgments** We acknowledge the use of HPC Cluster of Tianhe II in National Supercomputing Center in Guangzhou.

- 
- [1] S. Navas *et al.* [Particle Data Group], “Review of particle physics,” *Phys. Rev. D* **110**, no.3, 030001 (2024)
- [2] J. Lesgourgues and S. Pastor, “Massive neutrinos and cosmology,” *Phys. Rept.* **429**, 307-379 (2006) [arXiv:astro-ph/0603494 [astro-ph]].
- [3] N. Aghanim *et al.* [Planck], “Planck 2018 results. VI. Cosmological parameters,” *Astron. Astrophys.* **641**, A6 (2020) [erratum: *Astron. Astrophys.* **652**, C4 (2021)] [arXiv:1807.06209 [astro-ph.CO]].
- [4] M. Abdul Karim *et al.* [DESI], “DESI DR2 results. II. Measurements of baryon acoustic oscillations and cosmological constraints,” *Phys. Rev. D* **112**, no.8, 083515 (2025) [arXiv:2503.14738 [astro-ph.CO]].
- [5] S. Chabanier, M. Millea and N. Palanque-Delabrouille, “Matter power spectrum: from Ly $\alpha$  forest to CMB scales,” *Mon. Not. Roy. Astron. Soc.* **489**, no.2, 2247-2253 (2019) [arXiv:1905.08103 [astro-ph.CO]].
- [6] T. Louis *et al.* [Atacama Cosmology Telescope], “The Atacama Cosmology Telescope: DR6 power spectra, likelihoods and  $\Lambda$ CDM parameters,” *JCAP* **11**, 062 (2025) [arXiv:2503.14452 [astro-ph.CO]].
- [7] C. Garcia-Quintero *et al.* [DESI], “Cosmological implications of DESI DR2 BAO measurements in light of the latest ACT DR6 CMB data,” *Phys. Rev. D* **112**, no.8, 083529 (2025) [arXiv:2504.18464 [astro-ph.CO]].
- [8] E. Camphuis *et al.* [SPT-3G], “SPT-3G D1: CMB temperature and polarization power spectra and cosmology from 2019 and 2020 observations of the SPT-3G Main field,” [arXiv:2506.20707 [astro-ph.CO]].
- [9] Q. G. Huang, K. Wang and S. Wang, “Constraints on the neutrino mass and mass hierarchy from cosmological observations,” *Eur. Phys. J. C* **76**, no.9, 489 (2016) [arXiv:1512.05899 [astro-ph.CO]].
- [10] K. Cramer, J. Brehmer and G. Louppe, “The frontier of simulation-based inference,” *Proc. Nat. Acad. Sci.* **117**, no.48, 30055-30062 (2020) [arXiv:1911.01429 [stat.ML]].
- [11] E. Castorina, C. Carbone, J. Bel, E. Sefusatti and K. Dolag, “DEMNUi: The clustering of large-scale structures in the presence of massive neutrinos,” *JCAP* **07**, 043 (2015) [arXiv:1505.07148 [astro-ph.CO]].
- [12] J. Liu, S. Bird, J. M. Z. Matilla, J. C. Hill, Z. Haiman, M. S. Madhavacheril, A. Petri and D. N. Spergel, “MassiveNuS: Cosmological Massive Neutrino Simulations,” *JCAP* **03**, 049 (2018) [arXiv:1711.10524 [astro-ph.CO]].
- [13] F. Villaescusa-Navarro, C. Hahn, E. Massara, A. Banerjee, A. M. Delgado, D. K. Ramanah, T. Charnock, E. Giusarma, Y. Li and E. Allys, *et al.* “The Quijote simulations,” *Astrophys. J. Suppl.* **250**, no.1, 2 (2020) [arXiv:1909.05273 [astro-ph.CO]].
- [14] C. Hahn, M. Eickenberg, S. Ho, J. Hou, P. Lemos, E. Massara, C. Modi, A. Moradinezhad Dizgah, B. R. S. Blancard and M. M. Abidi, “SimBIG: mock challenge for a forward modeling approach to galaxy clustering,” *JCAP* **04**, 010 (2023) [arXiv:2211.00660 [astro-ph.CO]].
- [15] C. Hahn *et al.* [SimBIG], “Cosmological constraints from the nonlinear galaxy bispectrum,” *Phys. Rev. D* **109**, no.8, 083534 (2024) [arXiv:2310.15243 [astro-ph.CO]].
- [16] E. Massara, C. Hahn, M. Eickenberg, S. Ho, J. Hou, P. Lemos, C. Modi, A. Moradinezhad Dizgah, L. Parker and B. R. S. Blancard, “Cosmological constraints using simulation-based inference of galaxy clustering with marked power spectra,” *Phys. Rev. D* **112**, no.8, 083507 (2025) [arXiv:2404.04228 [astro-ph.CO]].
- [17] J. Hou, A. Moradinezhad Dizgah, C. Hahn, M. Eickenberg, S. Ho, P. Lemos, E. Massara, C. Modi, L. Parker and B. R. S. Blancard, “Cosmological constraints from the redshift-space galaxy skew spectra,” *Phys. Rev. D* **109**, no.10, 103528 (2024) [arXiv:2401.15074 [astro-ph.CO]].
- [18] B. R. S. Blancard *et al.* [SimBIG], “Galaxy clustering analysis with SimBIG and the wavelet scattering transform,” *Phys. Rev. D* **109**, no.8, 083535 (2024) [arXiv:2310.15250 [astro-ph.CO]].
- [19] P. Lemos *et al.* [SimBIG], “Field-level simulation-based inference of galaxy clustering with convolutional neural networks,” *Phys. Rev. D* **109**, no.8, 083536 (2024) [arXiv:2310.15256 [astro-ph.CO]].
- [20] D. Blas, J. Lesgourgues and T. Tram, “The Cosmic Linear Anisotropy Solving System (CLASS) II: Approximation schemes,” *JCAP* **07**, 034 (2011) [arXiv:1104.2933 [astro-ph.CO]].
- [21] A. Lewis, A. Challinor and A. Lasenby, “Efficient computation of CMB anisotropies in closed FRW models,” *Astrophys. J.* **538**, 473-476 (2000) [arXiv:astro-ph/9911177 [astro-ph]].
- [22] A. Cole, B. K. Miller, S. J. Witte, M. X. Cai, M. W. Grootes, F. Nattino and C. Weniger, “Fast and credible likelihood-free cosmology with truncated marginal neural ratio estimation,” *JCAP* **09**, 004 (2022) [arXiv:2111.08030 [astro-ph.CO]].
- [23] L. Thiele, E. Massara, A. Pisani, C. Hahn, D. N. Spergel, S. Ho and B. Wandelt, “Neutrino Mass Constraint from an Implicit Likelihood Analysis of BOSS Voids,” *Astrophys. J.* **969**, no.2, 89 (2024) [arXiv:2307.07555 [astro-ph.CO]].
- [24] R. Jimenez, T. Kitching, C. Pena-Garay and L. Verde, “Can we measure the neutrino mass hierarchy in the

- sky?," JCAP **05**, 035 (2010) [arXiv:1003.5918 [astro-ph.CO]].
- [25] L. Xu and Q. G. Huang, "Detecting the Neutrinos Mass Hierarchy from Cosmological Data," Sci. China Phys. Mech. Astron. **61**, no.3, 039521 (2018) [arXiv:1611.05178 [astro-ph.CO]].
- [26] E. Di Valentino *et al.* [CORE], "Exploring cosmic origins with CORE: Cosmological parameters," JCAP **04**, 017 (2018) [arXiv:1612.00021 [astro-ph.CO]].
- [27] B. Audren, J. Lesgourgues, K. Benabed and S. Prunet, "Conservative Constraints on Early Cosmology: an illustration of the Monte Python cosmological parameter inference code," JCAP **02**, 001 (2013) [arXiv:1210.7183 [astro-ph.CO]].
- [28] W. J. Percival and M. L. Brown, "Likelihood methods for the combined analysis of CMB temperature and polarization power spectra," Mon. Not. Roy. Astron. Soc. **372**, 1104-1116 (2006) [arXiv:astro-ph/0604547 [astro-ph]].
- [29] <https://pla.esac.esa.int/pla/#cosmology>.
- [30] M. Ho, D. J. Bartlett, N. Chartier, C. Cuesta-Lazaro, S. Ding, A. Lapel, P. Lemos, C. C. Lovell, T. L. Makiinen and C. Modi, *et al.* "LtU-ILI: An All-in-One Framework for Implicit Inference in Astrophysics and Cosmology," Open J. Astrophys. **7**, 001c.120559 (2024) [arXiv:2402.05137 [astro-ph.IM]].
- [31] A. Tejero-Cantero *et al.*, "sbi: A toolkit for simulation-based inference," Journal of Open Source Software, **5**, no.52, 2505, (2020) [arXiv:2007.09114 [cs.LG]].
- [32] A. Paszke *et al.*, "PyTorch: An Imperative Style, High-Performance Deep Learning Library," [arXiv:1912.01703 [cs.LG]].
- [33] J. Alsing, B. Wandelt and S. Feeney, "Massive optimal data compression and density estimation for scalable, likelihood-free inference in cosmology," Mon. Not. Roy. Astron. Soc. **477**, no.3, 2874-2885 (2018) [arXiv:1801.01497 [astro-ph.CO]].
- [34] G. Papamakarios, "Neural Density Estimation and Likelihood-free Inference," [arXiv:1910.13233 [stat.ML]].
- [35] G. Papamakarios, T. Pavlakou and I. Murray, "Masked Autoregressive Flow for Density Estimation," [arXiv:1705.07057 [stat.ML]].
- [36] D. Foreman-Mackey, D. W. Hogg, D. Lang and J. Goodman, "emcee: The MCMC Hammer," Publ. Astron. Soc. Pac. **125**, 306-312 (2013) [arXiv:1202.3665 [astro-ph.IM]].
- [37] N. Aghanim *et al.* [Planck], "Planck 2018 results. VIII. Gravitational lensing," Astron. Astrophys. **641**, A8 (2020) [arXiv:1807.06210 [astro-ph.CO]].
- [38] Y. Akrami *et al.* [Planck], "Planck 2018 results. IX. Constraints on primordial non-Gaussianity," Astron. Astrophys. **641**, A9 (2020) [arXiv:1905.05697 [astro-ph.CO]].
- [39] M. White, R. Zhou, J. DeRose, S. Ferraro, S. F. Chen, N. Kokron, S. Bailey, D. Brooks, J. Garcia-Bellido and J. Guy, *et al.* "Cosmological constraints from the tomographic cross-correlation of DESI Luminous Red Galaxies and Planck CMB lensing," JCAP **02**, no.02, 007 (2022) [arXiv:2111.09898 [astro-ph.CO]].
- [40] F. Verdiani, L. Harscouet, M. Zennaro, D. Alonso and B. Hadzhiyska, "Cosmological constraints from the angular power spectrum and bispectrum of luminous red galaxies and CMB lensing," [arXiv:2510.17796 [astro-ph.CO]].
- [41] G. Franco Abellán, N. Anau Montel, O. Savchenko and C. Weniger, "How to embed any likelihood into simulation-based inference: Application to Planck and stage IV galaxy surveys and dynamical dark energy," Phys. Rev. D **112**, no.10, 10 (2025) [arXiv:2507.22990 [astro-ph.CO]].